PPPL-2193

UC20-F

178/3-26-85 JS (2)

DR-0892-3

I-20163

PPPL-2193

CONF-840910--25

CONFINEMENT STUDIES OF OHMICALLY HEATED PLASMAS IN TFTR

By

P.C. Efthimion et al.

MARCH 1985

PLASMA PHYSICS LABORATORY

NOTICE

Printed in the United States of America

Available from:

National Technical Information Service
U.S. Department of Commerce
5285 Port Royal Road
Springfield, Virginia 22161

Price Printed Copy $ __*__ ; Microfiche $4.50

*Pages	NTIS Selling Price
1-25	$7.00
25-50	$8.50
51-75	$10.00
76-100	$11.50
101-125	$13.00
126-150	$14.50
151-175	$16.00
176-200	$17.50
201-225	$19.00
226-250	$20.50
251-275	$22.00
276-300	$23.50
301-325	$25.00
326-350	$26.50
351-375	$28.00
376-400	$29.50
401-425	$31.00
426-450	$32.50
451-475	$34.00
476-500	$35.50
500-525	$37.00
526-550	$38.50
551-575	$40.00
567-600	$41.50

For documents over 600 pages, add $1.50 for each additional 25-page increment.

PPPL--2193

DE85 008718

CONFINEMENT STUDIES OF OHMICALLY HEATED PLASMAS IN TFTR

P.C. Efthimion, N.L. Bretz, M.G. Bell, M. Bitter, W.R. Blanchard, F. Boody, D. Boyd[a], C.E. Bush[b], J.L. Cecchi, J. Coonrod, S.L. Davis, D.L. Dimock, H.F. Dylla, S. von Goeler, R.J. Goldston, B. Grek, D.J. Grove, R.J. Hawryluk, H.W. Hendel, K.W. Hill, R. Hulse, D. Johnson, L.C. Johnson, R. Kaita, S.M. Kaye, M. Kikuchi[c], S.J. Kilpatrick, J. Kiraly[d], R.J. Knize, P.H. LaMarche, R. Little, D.M. Manos, M.P. McCarthy, D.C. McCune, K. McGuire, D.M. Meade, S.S. Medley, D.R. Mikkelsen, D. Mueller, M. Murakami[b], E.B. Nieschmidt[e], D.K. Owens, A.T. Ramsey, A.L. Roquemore, N.R. Sauthoff, J.F. Schivell, J-L. Schwob, S.D. Scott[b], S. Sesnic, J.C. Sinnis, F.J. Stauffer[a], J.D. Strachan, S. Suckewer, G.D. Tait, M. Tavernier[f], G. Taylor, F.H. Tenney, H.H. Towner, M. Ulrickson, K-L. Wong, A. Wouters, H. Yamada[g], K.M. Young, and M.C. Zarnstorff.

Plasma Physics Laboratory
Princeton University
Princeton, New Jersey 08544 USA

ABSTRACT

Systematic scans of density in large deuterium plasmas ($a = 0.83$ m) at several values of plasma current and toroidal magnetic field strength indicate that the total energy confinement time, τ_E, is proportional to the line-average density $\bar{n}_e$ and the limiter q. Confinement times of ~ 0.3 s have been observed for $\bar{n}_e = 2.8 \times 10^{19}$ m^{-3}. Plasma size scaling experiments with plasmas of minor radii a = 0.83, 0.69, 0.55, and 0.41 m at constant limiter q reveal a confinement dependence on minor radius weaker than $a^{1.1}$. The major-radius dependence of τ_E, based on a comparison between TFTR and PLT results, is consistent with R^2 scaling. From the power balance, the thermal diffusivity χ_e is found to be significantly less than the INTOR value. In the a = 0.41 m plasmas, saturation of confinement is due to neoclassical ion conduction (χ_i neoclassical >> χ_e).

[a]Permanent address: University of Maryland
[b]Permanent address: Oak Ridge National Laboratory, Oak Ridge, TN.
[c]Permanent address: Japan Atomic Energy Research Institute, Japan.
[d]Permanent address: Institute of Isotopes of the Hungarian Academy of Sciences, Budapest, Hungary
[e]Permanent address: EG&G Idaho, Inc.
[f]Permanent address: Université de Paris, Institut Curie, Paris, France.
[g]Permanent address: University of Tokyo, Japan.

Presented at the Tenth International Conference on Plasma Physics and Controlled Nuclear Fusion Research, London, UK, 12-19 September 1984

INTRODUCTION

The research goal of TFTR is to achieve and study tokamak plasmas at reactor-relevant parameters ($T_i \sim 10$ keV, $\bar{n}_e \sim 10^{20}$ m^{-3}). In order to generate such plasmas, 27 MW of deuterium neutral beam heating will be provided at a full energy of 120 keV with a pulse duration of 0.5 - 2.0 s duration. Adiabatic compression of beam-heated plasmas can also be used to maximize the plasma pressure. The ohmic heating studies in deuterium plasmas presented here provide an initial reference point for the subsequent study of neutral beam heated plasmas.

The Tokamak Fusion Test Reactor (TFTR) achieved first plasma in December, 1982. Since then, plasma experiments have been conducted in parallel with commissioning and testing of major tokamak components. In previous reports, the initial operation of TFTR has been described by Young et al. [1]. The initial confinement results have been reported by Efthimion et al. [2], and the experimental results during higher-powered ohmic heating, ending in January 1984, have been presented by Hawryluk et al. [3]. This paper reviews the present status of TFTR in regard to the confinement studies of ohmically heated plasmas.

The experiments have focussed on determining the dependence of confinement and impurity behaviour on the plasma density, limiter q, and plasma size. The density, current, and toroidal field dependences have been studied in the largest minor radius plasma (a = 0.83 m) over a current range I_p = 0.6 - 1.4 MA, a line-average density range $\bar{n}_e$ = 0.8 - 3.35 x 10^{19} m^{-3}, and toroidal magnetic field values (1.8 and 2.7 T) corresponding to a limiter q range of 2.3 - 6.2 where $q = 5B_\phi a^2/RI_p$. The plasma size scaling experiments concentrated on plasmas with minor radii of a = 0.83, 0.69, 0.55, and 0.41 m at a fixed major radius R ≈ 2.55 - 2.65 m and q ≈ 2.7 - 3.3. The smallest plasma studied has a = 0.41 m and R = 2.65 m which may be compared to PLT plasmas with a = 0.4 m and R = 1.3 m, in order to infer a dependence of the total energy confinement time on the major radius.

MACHINE STATUS

The TFTR presently operates at plasma currents up to I_p = 1.4 MA, toroidal fields up to B_ϕ = 2.7 T, and plasma durations up to 4 s [1,3]. The moveable limiter consists of three water-cooled Inconel blades covered with graphite tiles [4]. The limiter provides the wide range in the plasma minor and major radii necessary to study confinement size scaling. In particular, at a major radius of 2.55 m the available minor radius range is a = 0.3 - 0.83 m.

The initial conditioning of the vessel for the summer 1984 operational period was similar to the procedure used previously for the initial ohmic heating optimization. This procedure is described in detail by Dylla [5]. The conditioning for the summer 1984 operational period involved a two-week bakeout of the entire torus, including the pumping ducts, at 150°C. While the vessel was hot, 50 hours of glow discharge cleaning (p = 0.7 Pa, I ≈ 15 A) and 70 hours (45,000 pulses) of pulse discharge cleaning were performed. All discharge cleaning was done in hydrogen, except the last 12 hours, which was performed in deuterium. The only significant modifications to the internal vacuum vessel hardware prior to the summer operational period were the installation of graphite protective plates for two neutral beam lines and the removal of the TiC coating from the graphite limiter. The coating was removed because sections of the surface were damaged during the winter run period.

One of the remarkable operational characteristics of TFTR is the relatively small gas flow required to fuel the discharge. It is standard operating practice to initiate TFTR plasmas with a prefill pressure in the range of 3 - 4 x 10^{-3} Pa which requires a gas input of 2 - 3.5 x 10^{20} D-atoms depending on the programming and wall conditions. During the subsequent evolution of the discharge, the gas flow is controlled by a density feedback system. Typically, significant gas input is required only for the density-rise portions of the discharge ($t < 1.0$ s) and little or no additional gas input is required to maintain the plateau phase from 1.0 - 3.0 s. The total gas input required varies between 0.2 - 1.5 x 10^{21} D-atoms for the plasma density range of 0.2 - 4 x 10^{19} m^{-3}. The required gas input is linear with density over the explored range and varies between 1.0 and 1.4 times the number of electrons in the plasma volume. This variation is presumably a measure of changing recycling conditions.

Enhanced pumping speed is provided by ZrAl getter modules. With six modules the pumping speed was 110 m^3/s, compared with 10 m^3/s for the turbomolecular pumps. Although little systematic work has yet been done to assess the effectiveness of the getters, thus far there has been no observable change on the gas fueling rate, density limit, impurity concentration, or plasma confinement.

IMPURITIES AND RADIATION

For the winter 1983-1984 run period, the moveable graphite limiter was coated with TiC. Titanium was the major metallic impurity with a relative concentration of n_{Ti}/n_e as high as 5 x 10^{-3} in low density plasmas. Figure 1 shows a comparison of the metallic and low Z concentrations measured for the graphite and TiC coated limiter by X-ray pulse-height analysis as a function of density for I_p = 1.4 MA, a = 0.83 m, and R = 2.55 m. After the TiC was removed, the titanium was reduced a factor of 40. The nickel, from the Inconel inner wall limiter, increased modestly. However, all the metallic impurities decreased substantially at the higher densities. In contrast, the concentration of low Z ions showed no measurable change and did not have a strong variation with density

The removal of the titanium had a noticeable effect on the plasma Z_{eff}. A comparison of Z_{eff} measured by X-ray pulse-height analysis and visible bremsstrahlung is shown as a function of density for the 1.4 MA plasmas in Fig. 2. Also shown is Z_{eff} from the summer run period for the 1 MA plasmas. Both measurements indicate a significant reduction in Z_{eff} with the removal of the TiC coating at low densities. As reported by Hawryluk [3], Z_{eff} decreases with increased density and minor radius and increases with increased plasma current. This trend is observed for all density and current scans. Regression fits indicate Z_{eff} is approximately proportional to the ratio of the average current density to the plasma density. Z_{eff} is as low as 2.5 - 3 at high density and currents of 1.0 - 1.4 MA. Impurity Z_{eff} measurements consistently lie between the estimates obtained from the Spitzer and neoclassical resistivity models.

The radiated power measured by the bolometer array has also changed with the removal of the titanium (Fig. 3). With the TiC coated graphite limiter, the total radiated power decreased with increasing density. With the coating removed, the total radiation for the 1.4 MA plasma was much lower (P_{rad}/P_{oh} ~ 0.6) at low density, increased with density, and eventually reached the same values obtained with the TiC coated graphite limiter (P_{rad}/P_{oh} ~ 0.8). The radiation profile with and without the coating was hollow, with the central radiation representing less than 10% of the central ohmic input power (using Spitzer resistivity to estimate the central current density). The radiated power density is equal to the input power density at r/a = 0.6 - 0.7.

CONFINEMENT STUDIES

The energy confinement time is evaluated at the end of the current and density flattops (2.8 - 3.1 s). At this time all plasma discharges in TFTR reach equilibrium, and the surface voltage approaches a value in the range of 0.8 - 1.4 V, depending on the plasma parameters. The confinement time is calculated with either the time-dependent analysis code TRANSP or the time-independent equilibrium code SNAP. The total energy confinement time, τ_E, is defined by

$$\tau_E = \frac{(W_e + W_i)}{P_{oh} - \frac{d}{dt}(W_e + W_i)} ,$$

where W_e and W_i are the electron and ion stored energies and P_{oh} is the ohmic input power. The measured electron temperature profile, the line-integral density, the surface voltage, Z_{eff} (assumed independent of radius), the metallic contribution to Z_{eff}, the central ion temperature, the deuterium-hydrogen ratio, and the major and minor radii are inputs to both codes. Initially, the density profile is assumed to be parabolic; this assumption has a weak effect on the confinement times (< 10%) when constrained by the line-average density. Recently, this assumption has been shown to be consistent with Thomson scattering density profiles (Fig. 4). The power input to the ions is assumed to occur by means of Coulomb collisions with the electrons. The ion conduction is adjusted by using a constant multiplier on the neoclassical value in the power balance to make simulated diagnostic ion temperatures match the measured values from charge exchange or Doppler broadening of TiXXI Kα or the measured neutron yield.

Figure 4 compares electron temperature profiles obtained by Thomson scattering and electron cyclotron emission (scanning radiometer and Michelson interferometer) for a plasma with $\bar{n}_e = 2.7 \times 10^{19}\ m^{-3}$, $q = 2.3$, and $I_p = 1.4$ MA. The peak temperature value obtained from X-ray pulse-height analysis is included. Electron temperature profiles determined from the electron cyclotron emission were corrected for the contributions to the total magnetic field from the poloidal magnetic field and paramagnetism [6]. Temperature and density profiles are flat within the inversion radius of the sawteeth. As q decreases, the temperature profile broadens substantially. During the summer run period, position measurements based on temperature profile measurements agreed well with each other and were consistent with equilibrium magnetic measurements. These confinement results are known within ±12%. During the winter run, inconsistencies in position measurements had limited the accuracy to ±18 %.

All the ohmic discharges are dominated by sawtooth activity. For the lower current plasmas (I_p < 1.2 MA), the ordinary sawtooth has been observed. However, for the higher currents (I_p > 1.2 MA) enhanced sawteeth are observed with periods up to 0.09 s. Similar sawteeth have been observed on D-III [7] and TEXT [8]. From the time evolution of the electron temperature profile and X-ray emissivity, the large sawteeth show complete reconnection from the magnetic axis to the plasma periphery. During the relaxation, the electron temperature profile flattens or hollows.

Furthermore, there is a smaller, intermediate sawtooth which appears to be more limited in spatial extent. This activity is believed to be due to the transient existence of two $q = 1$ surfaces.

For the largest plasmas ($a = 0.83$ m, $R = 2.55$ m) density scans were conducted for plasma currents of $I_p = 0.6$, 0.8, 1.0, 1.2, and 1.4 MA at $B_\phi = 2.7$ T (Fig. 5). For any current the confinement time increases with density, reaching a maximum of 0.3 s. A maximum line-average density of $\bar{n}_e = 3.35 \times 10^{19}$ m^{-3} has been obtained. At fixed density the confinement time decreased with increasing current ($\tau_E \propto I_p^{-1.1}$). A limited number of discharges at $I_p = 0.8$ MA and $B_\phi = 1.8$ T indicated that the confinement time depends on q, rather than on the plasma current:

$$\tau_E \propto \bar{n}_e q^{1.1} \ .$$

The q dependence is similar to that observed in DIII [9]. Scans at 1.4 MA taken with the bare graphite limiter show a 20% improvement in the confinement time compared to the TiC coated limiter.

The contribution of ion transport to the power balance is known with less precision than the global confinement because the electron-ion temperature difference is not well known. Figure 6 illustrates some of these difficulties in a discharge with $\bar{n}_e = 2.7 \times 10^{19}$ m^{-3}. Both the ion and electron temperature measurements have a 10% uncertainty, but the uncertainty in the difference is greater than 50%. Assuming a particle confinement time of 0.2 s (neutral density, $n_0(0) = 10^{12}$ m^{-3}) and no increase in transport due to sawteeth in the center, the ion conduction is in the range 0-8 times neoclassical [10]. Sawtooth mixing of ion energy, simulated by the BALDUR code, predicts that $\langle T_e \rangle - \langle T_i \rangle$ can be 0.2 - 0.3 keV larger than the value that would result from neoclassical conduction alone. It is also important to recognize that the choice of τ_p determines the relative importance of conduction and convection in the ion power balance and is itself significantly responsible for the large uncertainty in the neoclassical multiplier.

PLASMA SIZE SCALING

The moveable limiter has been used to form plasmas of different minor radii. Density scans have been made for a = 0.83, 0.69, 0.55, and 0.41 m at R = 2.55 - 2.65 m, B_ϕ = 2.7 T, and q = 2.7 - 3.3. The density limit, radiation fraction and profile, Z_{eff} range, and electron temperature profile shape of all these discharges are similar. When $\bar{n}_e \leq 2 \times 10^{19}$ m^{-3}, the total energy confinement time is linear with density for plasmas of all sizes. However, both the a = 0.41 and 0.55 m plasmas show signs of saturating as $\bar{n}_e$ increases beyond this value. Figure 7 shows the gross energy confinement time as a function of $\bar{n}_e q$ for plasmas with radii a = 0.83, 0.55, and 0.41 m studied during the summer run period. Note that there are sets of points for the a = 0.83 m plasmas from the confinement analysis using the Thomson scattering temperature and density profiles, and from analysis using the scanning radiometer temperature profiles. The q dependence has been adopted from the studies of the a = 0.83 m plasmas. The q range for the smaller plasmas is limited (2.7 - 3.3). The inferred minor radius scaling depends on which minor radii plasmas are compared. The a = 0.83 and 0.55 m plasmas imply a very weak dependence ($\tau_E \propto a^{0.2}$) while the a = 0.55 m and 0.41 m discharges imply $\tau_E \propto a^{1.1}$. The weakening of the scaling for the larger plasmas is consistent with the size scaling experiments conducted last winter (Hawryluk et al. [3]) and may be related to the proximity of the plasma to the vessel wall for the larger plasmas, or to the greater relative importance of ion conduction in the smaller plasmas. A similar weakening of the a-scaling near the vessel wall has been observed by Ejima [9]. Comparing the 0.41 m TFTR plasmas with those from PLT [11] ($a = 0.4$ m, $R = 1.3$ m) implies $\tau_E/\bar{n}_e q \propto R^2$. However, the PLT data were taken at $q \approx 4 - 7$, and PLT confinement did not show a systematic variation with q.

In the 0.41 m plasmas, ion conduction is consistent with the neoclassical model at all densities. Because the electron-ion temperature difference is somewhat larger, smaller limits may be set on the neoclassical multiplier (1-3). Figure 8 shows the central power input available ($P_{oh} - P_{rad}$) for electron or ion conduction and convection. At low densities collisional coupling to ions is small, but at higher densities virtually all the power flows through the ion channel and one finds $\chi_i \gg \chi_e$. The range of uncertainty shown in $P_{ie}(0)$ represents 1-3 times the neoclassical multiplier and, in all cases, brackets the coupling inferred from the measured neutron flux (x's). Thus, the saturation in confinement with density is caused by ion transport, which we estimate to be dominated by conduction. Ion conduction is more apparent in the small plasmas because the electron conduction scales approximately as a, whereas ion conduction in the banana regime scales as $a^{-3/2}$. These results are similar to those of Ejima et al. [9], who see low neoclassical multipliers for small plasmas; however, density saturation is not seen in TFTR in the larger plasmas, in contrast to D-III results.

The combined confinement results from Figs. 5 and 7 are shown in Fig. 9, with the confinement time plotted as a function of $\bar{n}_e R^2 a q$. The confinement results of PLT are also included. This scaling is similar to that of Pfeiffer and Waltz [12] and Alcator [13], but the q dependence observed on TFTR is included. TFTR results are also consistent with the T-11 [14] scaling of $\tau_E \propto R^{2.5}a^{0.4}$.

ELECTRON THERMAL CONDUCTION

From the electron power balance, the electron thermal diffusivity, χ_e, can be calculated as a function of position where

$$\chi_e(r) = - \frac{\int_0^r [P_{oh}(r') - P_{rad}(r') - P_{ie}(r') - P_{conv}(r')]\, r'dr'}{n_e\, r\, \frac{d\,T_e}{d\,r}} ,$$

$P_{rad}(r)$ is the radiation power density, $P_{oh}(r)$ is the ohmic heating input power density to the electrons, and $P_{ie}(r)$ is the electron collisional heat loss to the ions. The convection power density $P_{conv}(r)$ has been calculated assuming a particle confinement time of 0.1 - 0.25 s and represents a small loss compared to conduction. Because significant temperature gradients exist only outside the q = 1 surface, χ_e has been calculated and averaged over the range $0.5a < r < 0.7a$. Figure 10 is a plot of the electron thermal diffusivity as a function of electron density for the large plasmas. For this analysis the ion power balance has been constrained to match the measured neutron emission. The diffusivity varies inversely with $\bar{n}_e$ and q, as shown by the family of curves of χ_e with constant q. The top curve is interesting because it is comprised of discharges with the same q, but different currents and toroidal fields (I_p = 0.8 MA, B_ϕ = 2.1 T, and I_p = 1.4 MA, B_ϕ = 2.7 T). The INTOR values are significantly greater than the χ_e values obtained from the power balance. One obtains a slightly different density dependence if the analysis uses neoclassical ion conduction. The data from Fig. 10 show $\chi_e \propto n_e^{-1.3}$ while $\chi_e \propto n_e^{-0.8}$ when neoclassical ion conduction is assumed. The electron diffusivity also decreases with a at constant q and R until its estimation becomes extremely difficult as ions begin to carry away most of the power.

SUMMARY

Experimental studies of ohmically heated plasmas in TFTR have focussed upon plasma optimization and plasma confinement. A maximum line-average density $\bar{n}_e$ = 3.35 x 10^{19} m^{-3} has been reached, and a total energy confinement time up to τ_E = 0.3 s has been observed. The confinement times increase with density and q. Z_{eff} varies systematically with $I_p/n_e a^2$ and at high density falls to values of 2.5 - 3.

In plasma size-scaling experiments comparing plasmas of different a at constant R, the minor radius dependence is weak ($\lesssim a^{1.1}$) and changes slightly depending on the size of the plasma being compared. When the a = 0.41 m TFTR plasma is compared to similar ones in PLT, a strong major radius dependence ($\propto R^2$) in confinement is deduced.

For all the large (a = 0.83 m) plasmas, the transport loss is dominated by the electrons. The electron thermal conductivity χ_e varies inversely with density, decreases with increasing q, and is significantly smaller than the INTOR values. There is evidence that neoclassical ion conduction dominates the transport in the smaller plasmas (a ≈ 0.41, 0.55 m) at their highest densities.

Future studies of ohmically heated plasmas will be conducted at different major radii (R = 2.1 - 3.1 m) to establish a major-radius dependence from the TFTR data. In addition, studies at a higher toroidal field will be conducted this fall (B_ϕ = 4.0 T) and next spring (B_ϕ = 5.2 T). Following present scaling laws, we would expect τ_E to rise to 0.5 - 0.6 s at $\bar{n}_e \approx 6.5 \times 10^{19}\ m^{-3}$ for constant q = 2.5 - 3.0.

ACKNOWLEDGMENTS

It is a pleasure to acknowledge the many engineers, computer programmers, technicians, and other staff members who have supported the TFTR program. We are grateful to Dr. H.P. Furth and Dr. P.H. Rutherford for their support. We regret the recent death of our colleague F. Tenney. This work was supported by U.S. DoE Contract No. DE-AC02-76-CHO-3073.

REFERENCES

[1] Young K.M., et al., Plasma Phys. 26 11 (1984).

[2] Efthimion P.C., et al., Phys. Rev. Lett., 52 1492 (1984).

[3] Hawryluk, R.J., et al., Proc. 4th Intl. Symp. on Heating in Toroidal Plasmas, Rome (Intl. School of Plasmas Physics, Varenna, 1984) p.1012.

[4] Cecchi, J.L., et al., J. Nucl. Mater., accepted for publication.

[5] Dylla, H.F., et al., *J. Vac. Sci. Technol.*, A2 1188 (1984).
Dylla, H.F., et al., J. Nucl. Mater., 128 & 129 (1984).

[6] Clark, W., Plasma Phys., 25 1501 (1983).

[7] Pfeiffer, W., et al., GA Technologies Report, GA-A116994 (1983).

[8] Snipes, J. et al., J. Bull. Am. Phys. Soc., 28 1034 (1983).

[9] Ejima, S., Nucl. Fusion, 22 1627 (1982).

[10] Chang, C.S. and Hinton, F.L., Phys. Fluids, 25 1493 (1982).

[11] Hawryluk, R.J., et al., Nucl. Fusion, 10 1307 (1979).

[12] Pfeiffer, W. and Waltz, R.E., Nucl. Fusion, 19 51 (1979).

[13] Blackwell, B., et al., in Plasma Physics and Controlled Nuclear Fusion, IAEA, Vienna, 1981, IAEA-CN-41/I-3 (1982).

[14] Leonov, V.M., et al., in Plasma Physics and Controlled Nuclear Fusion, IAEA, Vienna, 1981, Vol. I, p.393.

FIGURE CAPTIONS

FIG. 1 Comparison of relative concentration of the metallic and low Z ion impurities for the TiC coated graphite limiter and uncoated graphite limiter. The error bar represents the absolute accuracy of the measurements.

FIG. 2 Comparison of Z_{eff} measured by X-ray pulse-height analysis and visible bremsstrahlung as a function of density at I_p = 1.4 MA for the TiC coated graphite and the uncoated graphite limiter, as well as Z_{eff} for graphite limiter at I_p = 1.0 MA.

FIG. 3 Comparison of radiated power and ohmic input power for the TiC coated graphite limiter (open symbols) and the uncoated graphite limiter (closed symbols).

FIG. 4 Comparison of the electron temperature profiles measured by Thomson scattering and electron cyclotron emission (scanning radiometer and Michelson interferometer). Also included is the central temperature measured by X-ray pulse-height analysis and the Thomson scattering density profile (below).

FIG. 5 Total energy confinement time as a function of density in the large plasmas (a = 0.83 m, R = 2.55 m) for various currents and toroidal field strengths. The error bar represents the absolute accuracy in the confinement measurements.

FIG. 6 The time evolution of the central electron and ion temperatures measured by the various temperature diagnostics.

FIG. 7 The total energy confinement time vs. $\bar{n}_e q$ for plasmas with a = 0.83, 0.55, and 0.41 m. Note that there are sets of points for the a = 0.83 m plasmas from the confinement analysis using the Thomson scattering profiles and the analysis using scanning radiometer profiles.

FIG. 8 Central power densities for the a = 0.41 m plasmas. Neoclassical current density profile is assumed [q(o) = 0.8]. P_{ei} error bar limits indicate 1 and 3 times neoclassical. X's indicate value from matching the neutron emission.

FIG. 9 The total energy confinement time vs. $\bar{n}_e R^2 a q$ for the PLT and TFTR ohmic confinement results.

FIG. 10 The electron thermal diffusivity at r/a = 0.5 - 0.7 for the large plasmas at various q values, along with χ_e INTOR.

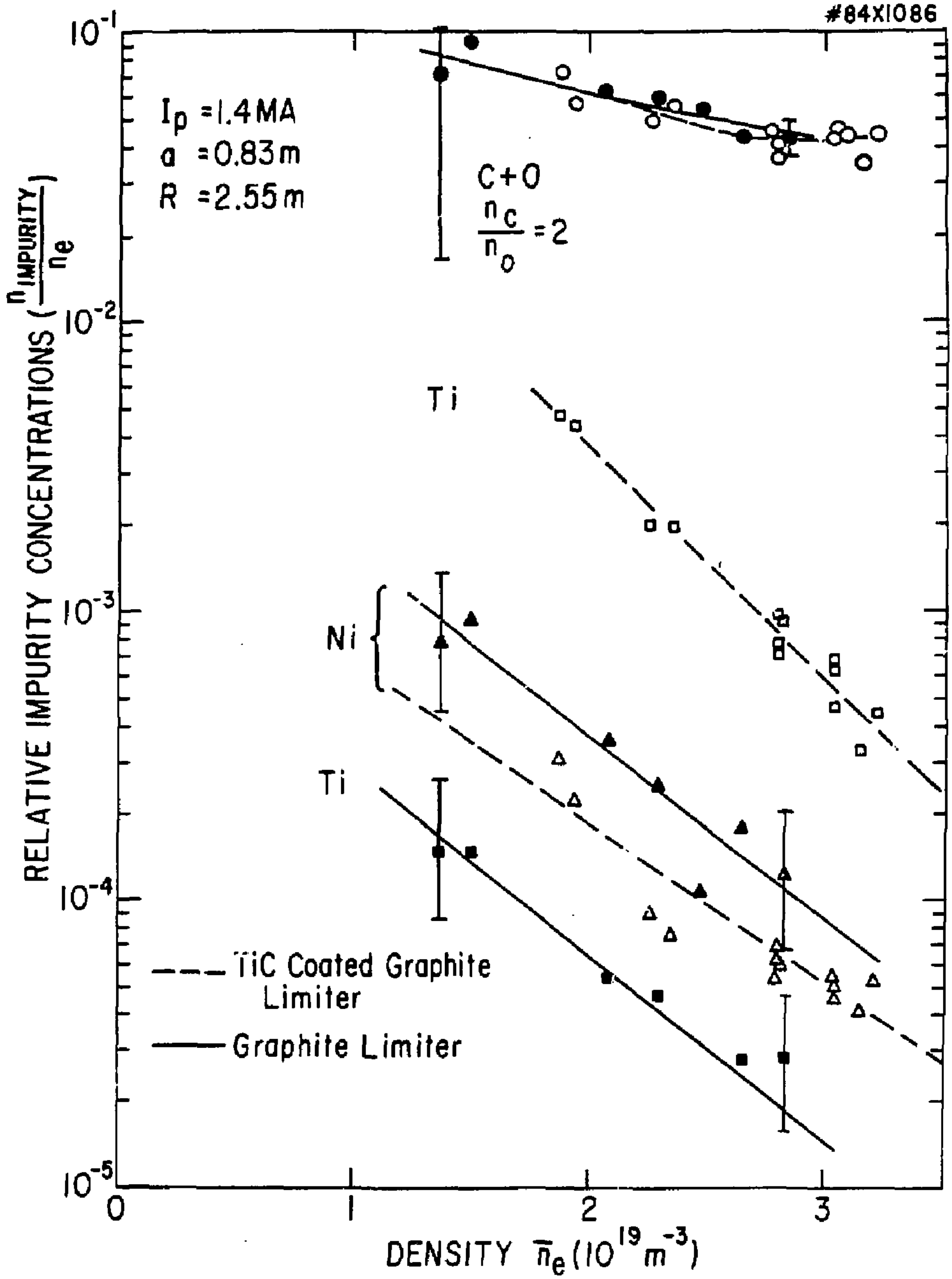
#84X1086
I_p =1.4MA
a =0.83m
R =2.55m
C+O
$\frac{n_C}{n_O}$ = 2
Ti
Ni
Ti
TiC Coated Graphite Limiter
Graphite Limiter
RELATIVE IMPURITY CONCENTRATIONS ($\frac{n_{IMPURITY}}{n_e}$)
DENSITY $\bar{n}_e (10^{19} m^{-3})$

Fig. 1

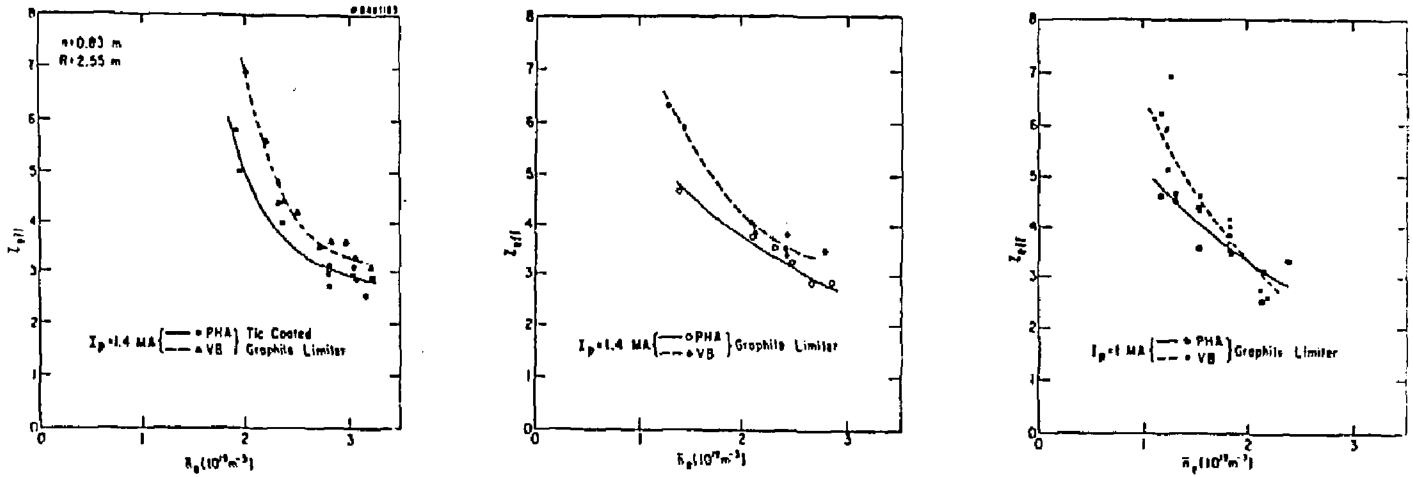
a=0.83 m
R=2.55 m
I_p=1.4 MA { PHA / VB } TiC Coated Graphite Limiter
Z_{eff}
$\bar{n}_e(10^{19}m^{-3})$
I_p=1.4 MA { PHA / VB } Graphite Limiter
Z_{eff}
$\bar{n}_e(10^{19}m^{-3})$
I_p=1 MA { PHA / VB } Graphite Limiter
Z_{eff}
$\bar{n}_e(10^{19}m^{-3})$

Fig. 2

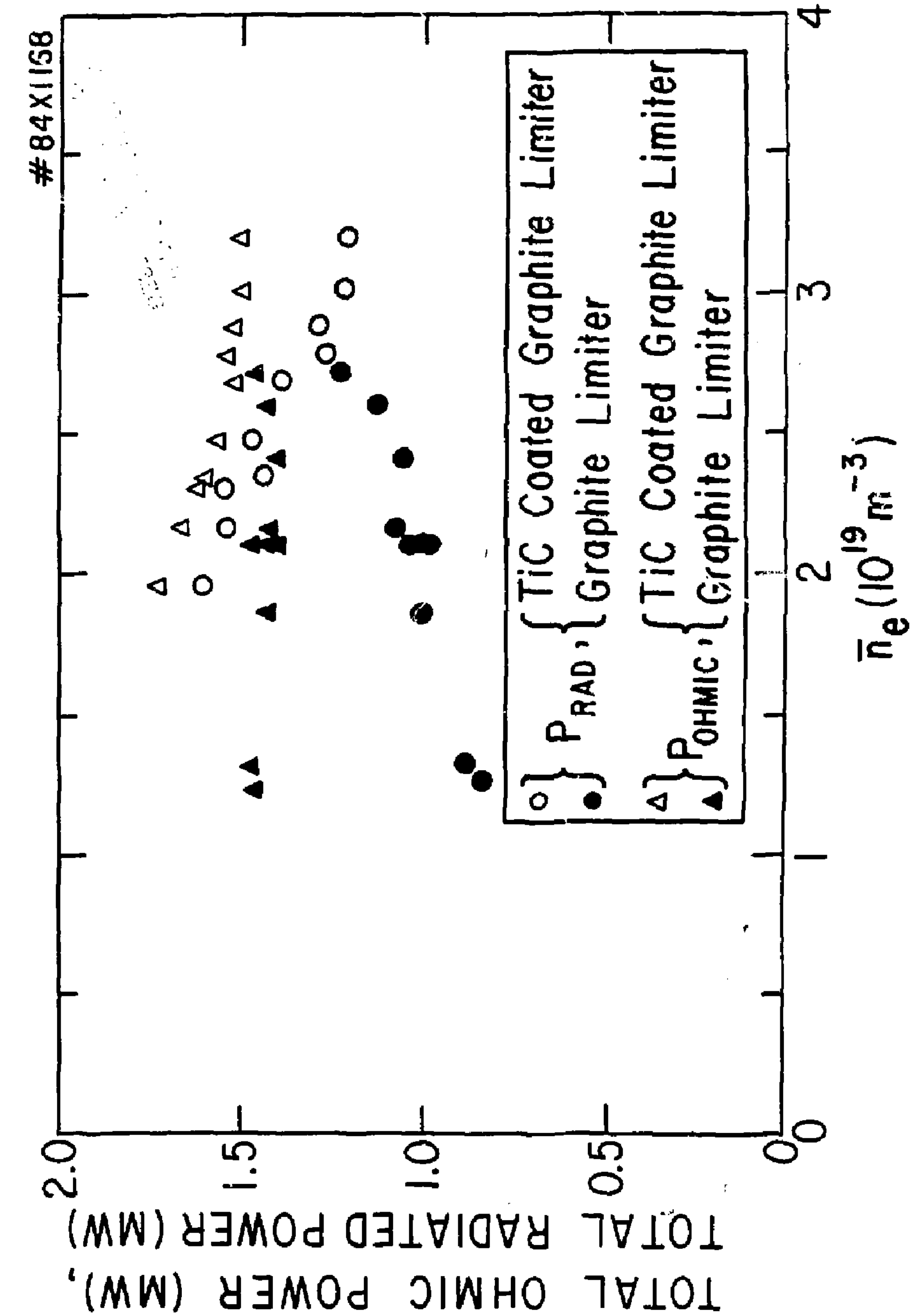
#84X1158
TOTAL OHMIC POWER (MW),
TOTAL RADIATED POWER (MW)
2.0
1.5
1.0
0.5
0
0
1
2
3
4
$\bar{n}_e (10^{19} m^{-3})$
P_{RAD}, TiC Coated Graphite Limiter
Graphite Limiter
P_{OHMIC}, TiC Coated Graphite Limiter
Graphite Limiter

Fig. 3

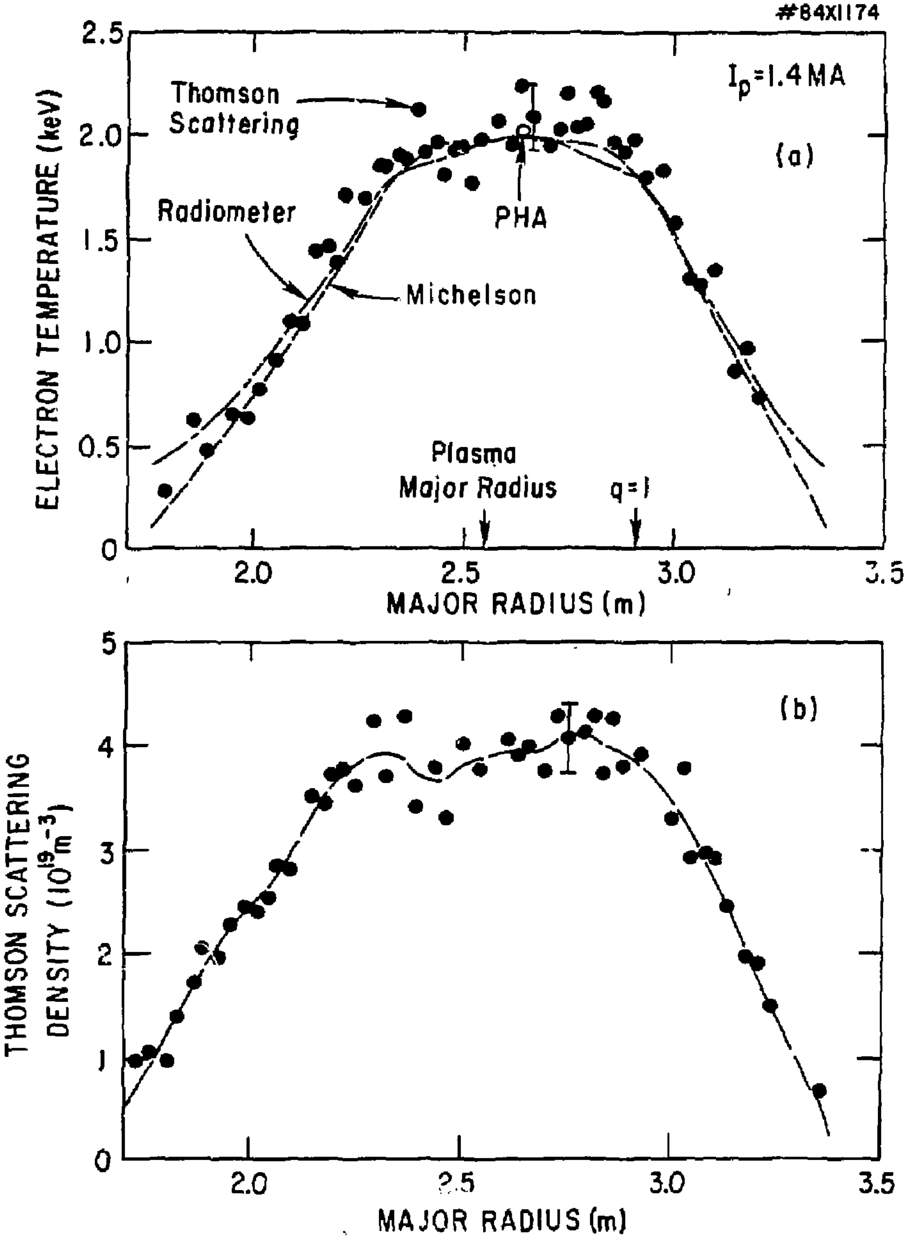
#84X1174
2.5
2.0
1.5
1.0
0.5
0
ELECTRON TEMPERATURE (keV)
Thomson Scattering
I_p=1.4 MA
(a)
Radiometer
Michelson
PHA
Plasma Major Radius
q=1
2.0
2.5
3.0
3.5
MAJOR RADIUS (m)
5
4
3
2
1
0
THOMSON SCATTERING DENSITY ($10^{19}m^{-3}$)
(b)
2.0
2.5
3.0
3.5
MAJOR RADIUS (m)

Fig. 4

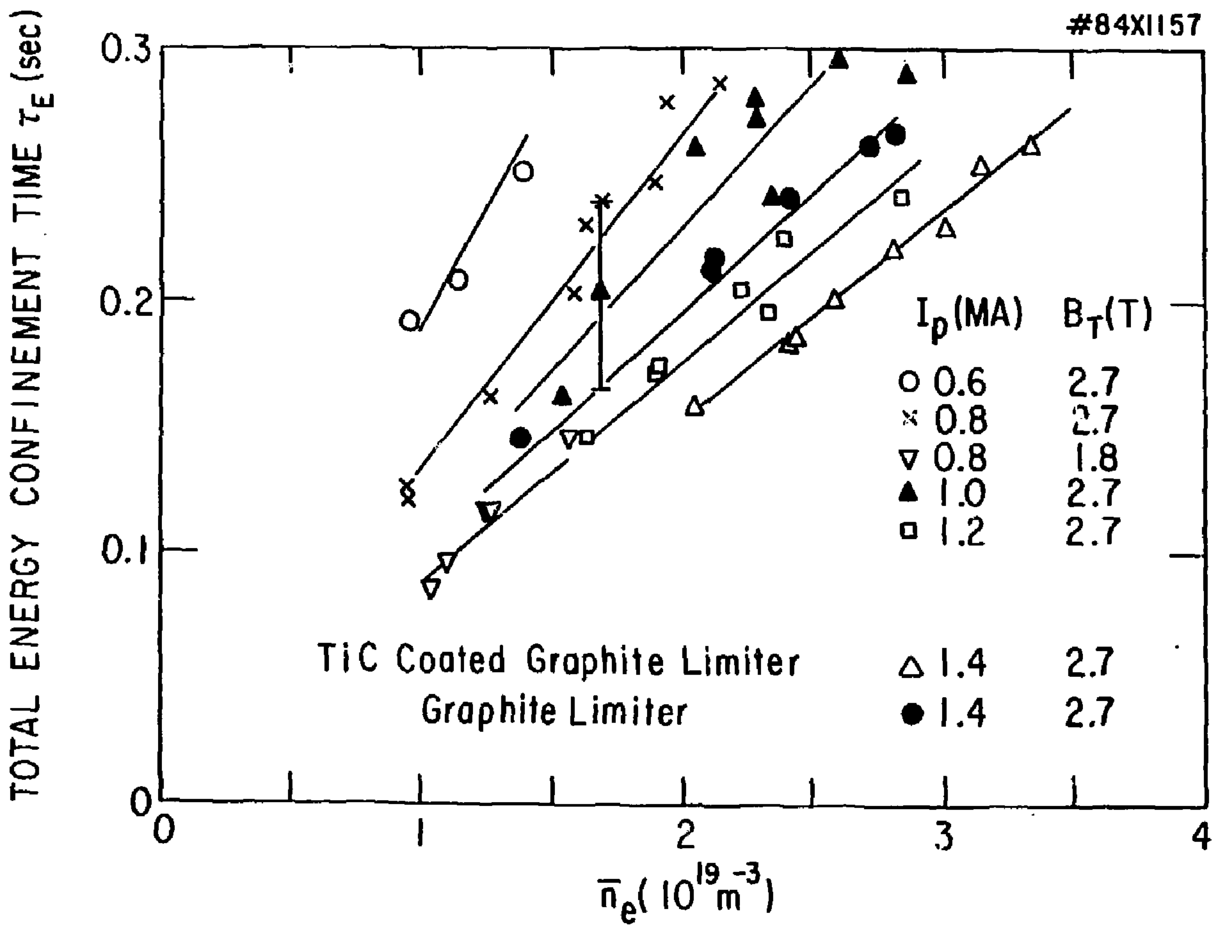

#84X1157
TOTAL ENERGY CONFINEMENT TIME τ_E (sec)
0.3
0.2
0.1
0
0
1
2
3
4
$\bar{n}_e (10^{19} m^{-3})$
I_p(MA) B_T(T)
○ 0.6 2.7
× 0.8 2.7
▽ 0.8 1.8
▲ 1.0 2.7
□ 1.2 2.7
TiC Coated Graphite Limiter △ 1.4 2.7
Graphite Limiter ● 1.4 2.7

Fig. 5

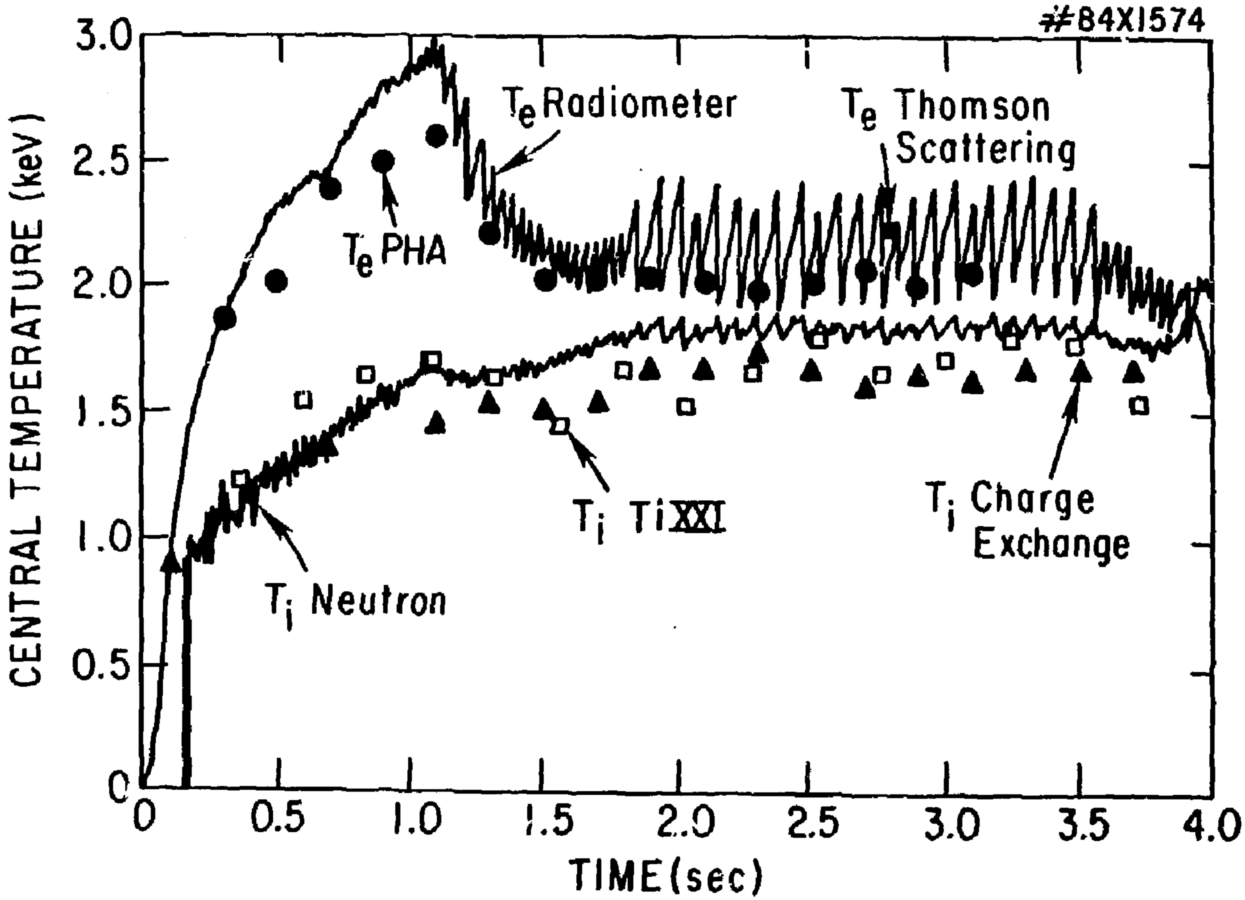
#84X1574
CENTRAL TEMPERATURE (keV)
3.0
2.5
2.0
1.5
1.0
0.5
0
0.5
1.0
1.5
2.0
2.5
3.0
3.5
4.0
TIME (sec)
Te Radiometer
Te PHA
Te Thomson Scattering
Ti Neutron
Ti TiXXI
Ti Charge Exchange

Fig. 6

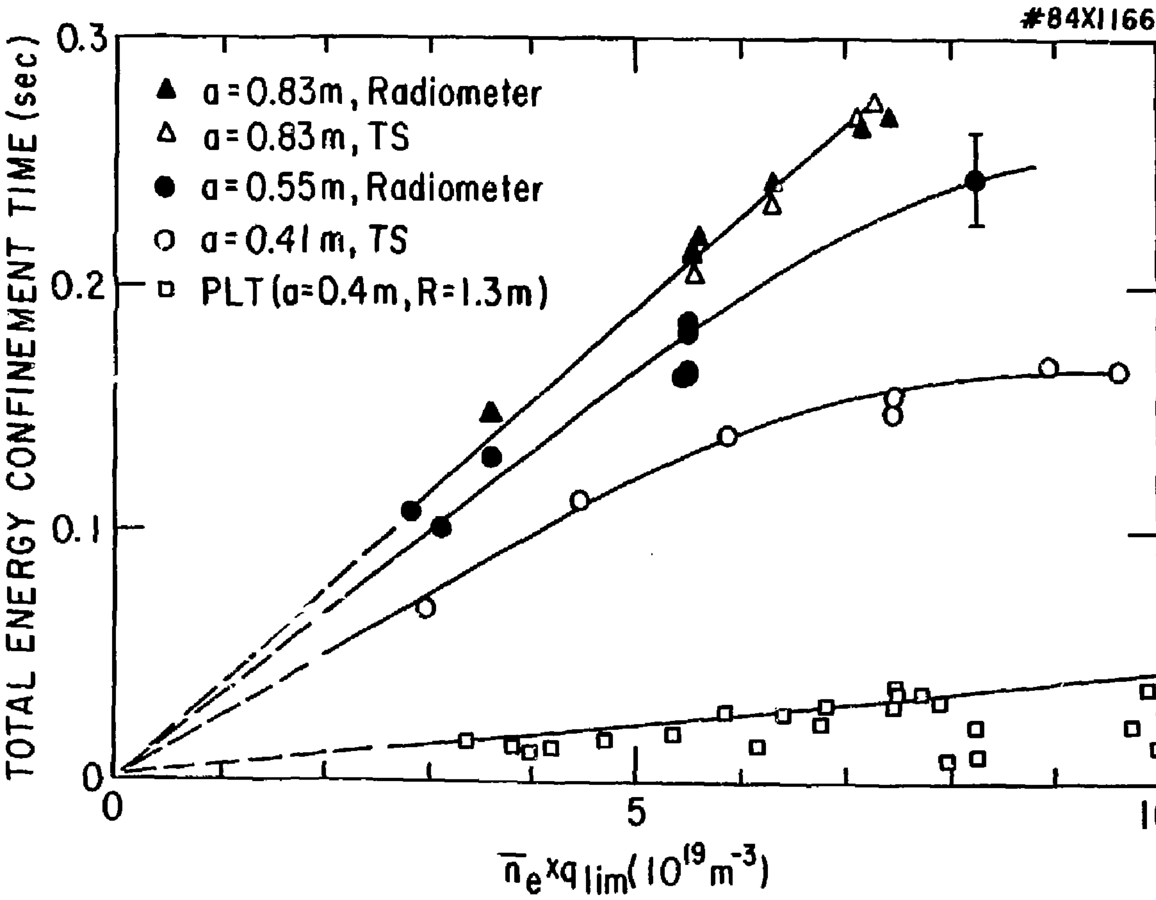
#84X1166
TOTAL ENERGY CONFINEMENT TIME (sec)
0.3
0.2
0.1
0
a=0.83m, Radiometer
a=0.83m, TS
a=0.55m, Radiometer
a=0.41m, TS
PLT(a=0.4m, R=1.3m)
0
5
10
$\overline{n}_e \times q_{lim} (10^{19} m^{-3})$

Fig. 7

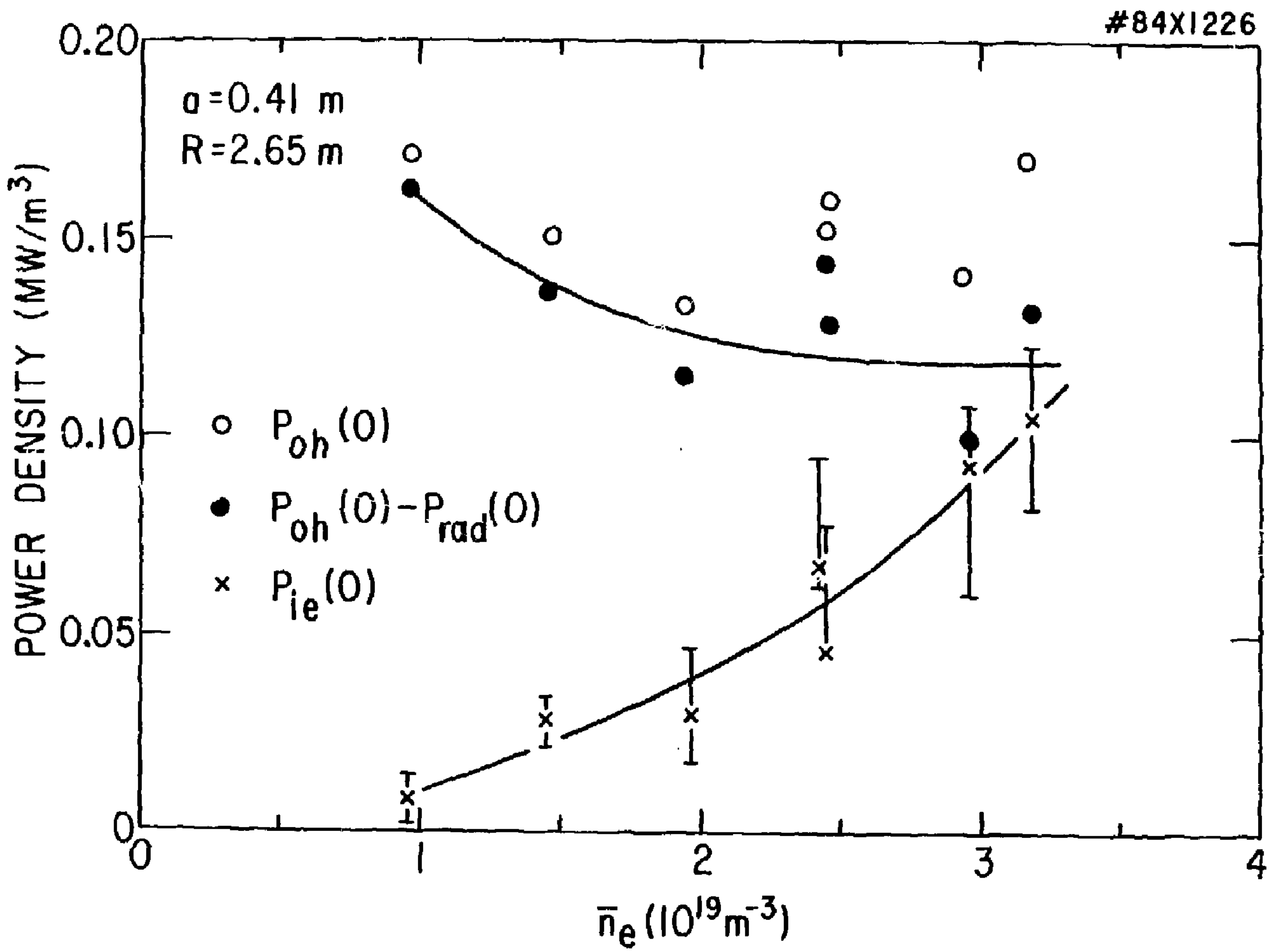
#84X1226
a=0.41 m
R=2.65 m
POWER DENSITY (MW/m³)
0.20
0.15
0.10
0.05
0
Poh(0)
Poh(0)−Prad(0)
Pie(0)
0
1
2
3
4
n̄e (10¹⁹ m⁻³)

Fig. 8

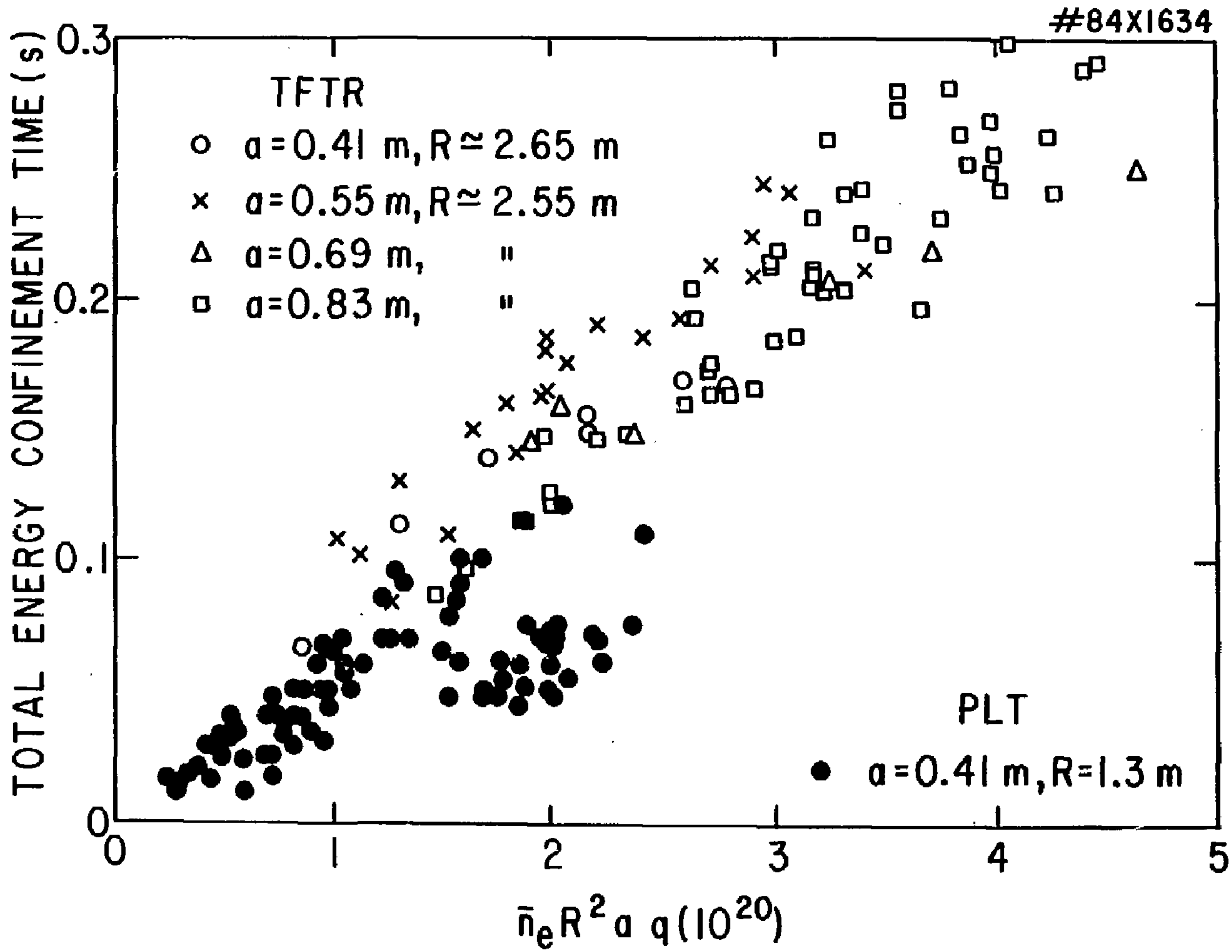

#84X1634
TOTAL ENERGY CONFINEMENT TIME (s)
0
0.1
0.2
0.3
TFTR
a=0.41 m, R≃2.65 m
a=0.55 m, R≃2.55 m
a=0.69 m, "
a=0.83 m, "
PLT
a=0.41 m, R=1.3 m
0
1
2
3
4
5
$\bar{n}_e R^2 a\, q\, (10^{20})$

Fig. 9

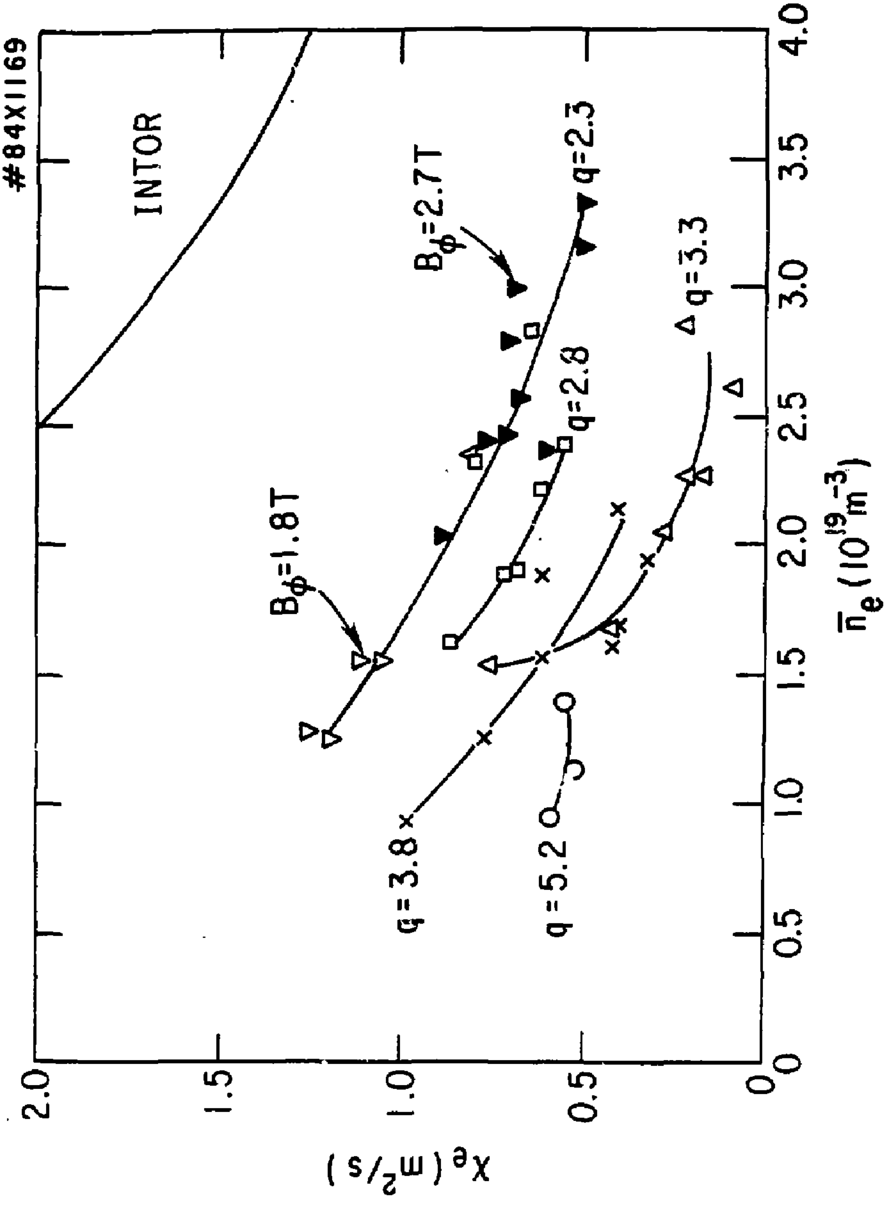

#84X1169
INTOR
B_ϕ=2.7T
q=2.3
q=2.8
q=3.3
B_ϕ=1.8T
q=3.8
q=5.2
χ_e (m^2/s)
$\bar{n}_e$ ($10^{19}m^{-3}$)
0
0.5
1.0
1.5
2.0
2.5
3.0
3.5
4.0

Fig. 10

EXTERNAL DISTRIBUTION IN ADDITION TO UC-20

Plasma Res Lab, Austra Nat'l Univ, AUSTRALIA
Dr. Frank J. Paoloni, Univ of Wollongong, AUSTRALIA
Prof. I.R. Jones, Flinders Univ., AUSTRALIA
Prof. M.H. Brennan, Univ Sydney, AUSTRALIA
Prof. F. Cap, Inst Theo Phys, AUSTRIA
Prof. Frank Verheest, Inst theoretische, BELGIUM
Dr. D. Palumbo, Dg XII Fusion Prog, BELGIUM
Ecole Royale Militaire, Lab de Phys Plasmas, BELGIUM
Dr. P.H. Sakanaka, Univ Estadual, BRAZIL
Dr. C.R. James, Univ of Alberta, CANADA
Prof. J. Teichmann, Univ of Montreal, CANADA
Dr. H.M. Skarsgard, Univ of Saskatchewan, CANADA
Prof. S.R. Sreenivasan, University of Calgary, CANADA
Prof. Tudor W. Johnston, INRS-Energie, CANADA
Dr. Hannes Barnard, Univ British Columbia, CANADA
Dr. M.P. Bachynski, MPB Technologies, Inc., CANADA
Chalk River, Nucl Lab, CANADA
Zhengwu Li, SW Inst Physics, CHINA
Library, Tsing Hua University, CHINA
Librarian, Institute of Physics, CHINA
Inst Plasma Phys, Academia Sinica, CHINA
Dr. Peter Lukac, Komenskeho Univ, CZECHOSLOVAKIA
The Librarian, Culham Laboratory, ENGLAND
Prof. Schatzman, Observatoire de Nice, FRANCE
J. Radet, CEN-BP6, FRANCE
AM Dupas Library, AM Dupas Library, FRANCE
Dr. Tom Mual, Academy Bibliographic, HONG KONG
Preprint Library, Cent Res Inst Phys, HUNGARY
Dr. S.K. Trehan, Panjab University, INDIA
Dr. Indra Mohan Lal Das, Banaras Hindu Univ, INDIA
Dr. L.K. Chavda, South Gujarat Univ, INDIA
Dr. R.K. Chhajlani, Vikram Univ. INDIA
Dr. B. Dasgupta, Saha Inst, INDIA
Dr. P. Kaw, Physical Research Lab, INDIA
Dr. Phillip Rosenau, Israel Inst Tech, ISRAEL
Prof. S. Cuperman, Tel Aviv University, ISRAEL
Prof. G. Rostagni, Univ Di Padova, ITALY
Librarian, Int'l Ctr Theo Phys, ITALY
Miss Clelia De Palo, Assoc EURATOM-ENEA, ITALY
Biblioteca, del CNR EURATOM, ITALY
Dr. H. Yamato, Toshiba Res & Dev, JAPAN
Direc. Dept. Lg. Tokamak Dev. JAERI, JAPAN
Prof. Nobuyuki Inoue, University of Tokyo, JAPAN
Research Info Center, Nagoya University, JAPAN
Prof. Kyoji Nishikawa, Univ of Hiroshima, JAPAN
Prof. Sigeru Mori, JAERI, JAPAN
Library, Kyoto University, JAPAN
Prof. Ichiro Kawakami, Nihon Univ, JAPAN
Prof. Satoshi Itoh, Kyushu University, JAPAN
Dr. D.I. Choi, Adv. Inst Sci & Tech, KOREA
Tech Info Division, KAERI, KOREA
Bibliotheek, Fom-Inst Voor Plasma, NETHERLANDS
Prof. B.S. Liley, University of Waikato, NEW ZEALAND
Prof. J.A.C. Cabral, Inst Superior Tecn, PORTUGAL
Dr. Octavian Petrus, ALI CUZA University, ROMANIA
Prof. M.A. Hellberg, University of Natal, SO AFRICA
Dr. Johan de Villiers, Plasma Physics, Nucor, SO AFRICA
Fusion Div. Library, JEN, SPAIN
Prof. Hans Wilhelmson, Chalmers Univ Tech, SWEDEN
Dr. Lennart Stenflo, University of UMEA, SWEDEN
Library, Royal Inst Tech, SWEDEN
Centre de Recherchesen, Ecole Polytech Fed, SWITZERLAND
Dr. V.T. Tolok, Kharkov Phys Tech Ins, USSR
Dr. D.D. Ryutov, Siberian Acad Sci, USSR
Dr. G.A. Eliseev, Kurchatov Institute, USSR
Dr. V.A. Glukhikh, Inst Electro-Physical, USSR
Institute Gen. Physics, USSR
Prof. T.J.M. Boyd, Univ College N Wales, WALES
Dr. K. Schindler, Ruhr Universitat, W. GERMANY
Nuclear Res Estab, Julich Ltd, W. GERMANY
Librarian, Max-Planck Institut, W. GERMANY
Bibliothek, Inst Plasmaforschung, W. GERMANY
Prof. R.K. Janev, Inst Phys, YUGOSLAVIA